nature neuroscience

Supplementary information

https://doi.org/10.1038/s41593-025-01945-y

# Autonomic physiological coupling of the global fMRI signal

In the format provided by the authors and unedited

## Supplementary Materials

### Supplementary Note 1 - MRI/EEG Acquisition Parameters Across Datasets

*ME-REST, ME-TASK, ME-TASK-CUE Data*

Detailed MRI/EEG acquisition parameters are provided in Goodale et al. [48]. Briefly, anatomical T1-weighted structural and multi-echo EPI functional scans were collected on a 3T Siemens Prisma scanner with a Siemens 64-channel head/neck coil. The multi-echo EPI sequence was acquired with TR = 2100 ms, echo times = 13.0, 29.4, and 45.7 ms, flip angle = 75 degrees, and voxel size = 3mm isotropic. The duration of the resting-state scan was 24.5 minutes, corresponding to a total of 700 volumes. The duration of the respiration task scan was slightly variable (14-15 minutes across subjects), corresponding to a total of 400-435 volumes, depending on the subject.

Simultaneous scalp EEG (sampling rate = 5 kHz) was acquired during the resting-state and respiration task using a 32-channel MR-compatible system. Photoplethysmography (PPG) and respiration belt signals (sampling rate: 2 kHz) were acquired during both the resting-state and respiration task sessions. The PPG transducer was placed on the left index finger. MRI scan triggers were recorded along with EEG and physiological signals for data synchronization.

*HCP-REST Data*

Detailed MRI/Physio acquisition parameters are provided in Smith et al. [68]. Briefly, resting-state fMRI scans were collected on Siemens 3T Tim Trio scanners with a multiband (factor of 8) accelerated EPI sequence with the following parameters: TR: 720ms, TE = 33.1ms, flip angle = 52 degrees, and voxel size= 2mm isotropic. Resting-state fMRI data was collected over two consecutive days for each subject and two sessions, each consisting of two 15-minute runs, amounting to four resting-state sessions per subject. Within a session, the two runs were acquired with opposite phase encoding directions: L/R encoding and R/L encoding. A single 15 min scan from each participant on the first day of scanning was selected. We balanced the number of L/R and R/L phase encoding scans across our participants (n=15 for L/R direction) to ensure results were not biased by acquisition from any given phase encoding direction. Photoplethysmography (PPG) and respiration belt signals (sampling rate = 400 Hz) were simultaneously acquired with resting-state EPI scans along with MRI scan triggers for data synchronization.

*NKI-REST and NKI-TASK Data*

Detailed acquisition parameters are provided on the Enhanced NKI-Rockland [50] webpage (http://fcon_1000.projects.nitrc.org/indi/enhanced/index.html). Briefly, resting-state and

breath hold fMRI scans were collected on a Siemens 3T Tim Trio scanner with a multiband (factor of 4) accelerated EPI sequence with the following parameters: TR = 1400ms, TE = 30ms, flip angle = 65 degrees, voxel size = 2mm isotropic. The duration of the resting-state scan was 10 minutes. The respiration task was a block design with the following sequence: 1) a 10-sec rest, 2) a 2-sec visual stimulus indicating the start of the trial (text: 'Get Ready'), 3) a 2-sec inhalation, 4) a 2-sec expiration, 5) a 2-sec deep inhalation, and 5) a breath hold for 18 secs. This sequence was repeated seven times, for a total duration of 4.5 minutes. PPG signals (recorded from the tip of the index finger), skin conductance (galvanic skin response; recorded from the hand), and respiration belt signals were simultaneously acquired with EPI scans along with MRI scan triggers for data synchronization.

*ME-REST-SUPP Data*

Detailed MRI acquisition parameters are provided in Spreng et al. [51]. Briefly, anatomical T1-weighted structural and multi-echo EPI functional scans were collected on a 3T GE Discovery MR750 scanner with a 32-channel head coil. The multi-echo EPI sequence was acquired with TR = 3000 ms, echo times = 13.7, 30, and 47 ms, flip angle = 83 degrees, and voxel size = 3mm isotropic. The duration of the resting-state scan was 10 minutes, corresponding to a total of 204 volumes. Photoplethysmography (PPG) and respiration belt signals (sampling rate: 40 or 50 Hz) were acquired during the session.

*YALE-REST Data*

Detailed MRI acquisition parameters are provided in Lee et al. [52]. Briefly, anatomical T1-weighted structural and single-echo, multiband EPI functional scans were collected on a MAGNETOM Prisma MRI scanner. The single-echo, multiband EPI sequence was acquired with TR = 1000ms, TE = 30ms, multiband acceleration factor = 5, flip angle = 55 degrees and voxel size = 2mm. The duration of each resting-state scan was 6 minutes and 50s. Simultaneous eye-tracking and pupil dilation was recorded using a MR-compatible infrared EyeLink 1000 Plus eye-tracking system with a 1000Hz sampling rate. We used minimally preprocessed pupil data provided by the authors for analysis (see details in *Methods and Materials*).

*NATVIEW-REST Data*

Detailed MRI/EEG acquisition parameters are provided in Telesford et al. [53]. Briefly, anatomical T1-weighted structural and single-echo EPI functional scans were collected on a 3T Siemens TIM Trio scanner with a 12-channel head coil. Resting-state EPI sequences were acquired with TR=2100ms, TE=2500ms, flip angle = 60 degrees, voxel size= ~3.5mm isotropic.

Simultaneous scalp EEG (sampling rate = 5 kHz) was collected using a customized 61-channel MR-compatible cap, including two electrooculogram (EOG) channels (above and below the left eye) and one electrocardiography (ECG) channel placed on the back. As with the *YALE-REST* dataset, simultaneous eye-tracking and pupil dilation was recorded using an MR-compatible infrared EyeLink 1000 Plus eye-tracking system with a 1000Hz sampling rate. We

used minimally preprocessed pupil data provided by the authors for analysis (see details below). Respiratory time courses were also collected with a respiratory belt, but due to data quality issues were not included in our analysis.

*Free Breathing and 'Clamped' CO2 Data*

Detailed MRI acquisition parameters are provided in Golestani & Chen [19]. Briefly, anatomical T1-weighted structural and single-echo, multiband EPI functional scans were collected on a Siemens TIM Trio 3T MRI scanner with a 32-channel head coil. Free-breathing and clamped CO2 fMRI recordings were acquired with TR = 380ms, TE = 30ms, multiband acceleration factor = 3, flip angle = 40 degrees and voxel size = 4x4x5 mm3.

**Supplementary Note 2 - MRI/EEG Preprocessing Pipeline Across Datasets**

*MRI Data Preprocessing*

Excluding the ME-REST, ME-TASK, ME-TASK-CUE and HCP-REST datasets, datasets were received in raw (unprocessed) NIFTI formats. Depending on the nature of the EPI functional acquisition, the nine datasets were processed with slightly different preprocessing pipelines. We first describe dataset-specific preprocessing, and then describe the common preprocessing steps that were applied to all datasets following dataset-specific preprocessing. All preprocessing steps were performed in either *Nipype* [69] with calls to *FSL* utilities.

*Dataset Specific Preprocessing*

For the ME-REST, ME-TASK, ME-TASK-CUE and ME-REST-SUPP datasets, multi-echo EPI functional preprocessing pipeline consisted of the following steps: the first 7 (ME-REST, ME-TASK, ME-TASK-CUE) and 4 (ME-REST-SUPP) volumes were removed, six-parameter rigid body motion correction and slice timing correction with *MCFLIRT* and *slicetimer* in FSL, respectively, Multi-Echo ICA denoising and optimal combination of echos using Tedana software (DuPre et al., 2020), non-linear registration to the MNI152 template using FSL's FMRIB's Nonlinear Image Registration Tool (FNIRT).

For the HCP-REST dataset, we used EPI functional scans previously preprocessed with the HCP's ICA-based artifact removal process [68] to minimize effects of spatially structured noise in our analysis. EPI scans were previously motion-corrected, registered to the MNI152 template, and intensity normalized. Comprehensive details of the HCP preprocessing pipeline are described in Glasser et al. (2013).

The NKI-REST, NKI-TASK, YALE-REST, NATVIEW-REST and clamped CO2 datasets shared a largely similar set of preprocessing steps. First, the first N volumes (~10s) of the NKI-REST (7), NKI-TASK (7), YALE-REST (10), and clamped CO2 (26) EPI functional scans were dropped to remove non-steady state time points. For the NATVIEW-REST dataset, the last 2 volumes were dropped to align with the EEG and pupillometry recordings (no volumes were dropped from the start of the scan). Slice timing correction was applied to the EPI functional scans of the NATVIEW-REST dataset using the *FSL slicetimer* utility due to its longer TR acquisition (TR=2.1s). Second, EPI functional scans from all datasets were motion corrected with six-parameter rigid body alignment with FSL *MCFLIRT.* EPI functional scans were then non-linearly registered to the MNI152 template using FSL's FMRIB's Nonlinear Image Registration Tool (FNIRT) [71].

*Common Preprocessing*

Following dataset-specific preprocessing, all datasets were then resampled to 3mm (isotropic) MNI152 space. Excluding the HCP-REST dataset, this resampling step occurred during FNIRT registration. For the clamped CO2 dataset, fMRI volumes were resampled to 4mm (isotropic) MNI152 space to more closely match its spatial sampling. Following resampling, fMRI volumes were spatially smoothed with a gaussian kernel (FWHM=5mm) and temporally filtered with a fifth-order Butterworth bandpass zero-phase filter (0.01-0.1Hz). For all datasets, voxels were extracted with a dilated MNI152 brain mask, so as to pick up voxel time courses in large dural venous sinuses and CSF compartments.

*EEG Preprocessing*

Preprocessing of EEG recordings in the ME-REST, ME-TASK and ME-TASK-CUE datasets are described in [48]. Briefly, channel time courses were first corrected for gradient artifacts through the average artifact subtraction method [72]. Ballistocardiogram artifacts were removed by subtraction of an average artifact template locked to cardiac R-peaks, followed by independent component analysis (ICA) of the template-subtracted time courses. The scalp EEG channel time courses were referenced to channel FCz for analysis.These EEG preprocessing steps were performed with the BrainVision Analyzer software.

Preprocessing of EEG recordings for the NATVIEW-REST dataset was performed with custom EEGLAB MATLAB scripts provided by the authors of the dataset (https://github.com/NathanKlineInstitute/NATVIEW_EEGFMRI) and are described in Telesford et al. [53]. Briefly, the preprocessing steps included 1) gradient artifact removal with the FASTR utility from the EEGLAB FMRIB Plugin, 2) QRS/heartbeat detection using the ECG channel, followed by pulse artifact correction with a template subtraction method, and 3) bandpass filtered between 0.3 to 50Hz using a Hamming windowed sinc FIR filter. Scalp EEG time courses were referenced to the common average for analysis.

**Supplementary Movies**

Supplementary Movie 1. **Temporal Reconstruction of CPC1 in ME-REST Dataset.**

Supplementary Movie 2. **Temporal Reconstruction of CPC1 in ME-REST-SUPP Dataset.**

Supplementary Movie 3. **Cross-Correlation of fMRI Signals and PPG Amplitude in ME-REST Dataset.**

Supplementary Movie 4. **Cross-Correlation of fMRI Signals and PPG Amplitude in ME-REST-SUPP Dataset.**

**Supplementary Tables**

| Dataset | Sample | Physio Signals Used | Source | Sample Size | Number of Sessions | Age Range | Sex (F) |
|---|---|---|---|---|---|---|---|
| ME-REST | Full | EEG, Respiration, PPG | Goodale et al. (2021). *ELife*. https://doi.org/10.7554/eLife.62376<br><br>https://doi.org/10.6084/m9.figshare.28225415.v3. | 11 | 15 | 21-35 | 6 |
| ME-TASK | Full | EEG, Respiration, PPG | https://doi.org/10.6084/m9.figshare.28225415.v3. | 6 | 9 | 22-57 | 4 |
| ME-TASK-CUE | Full | EEG, Respiration, PPG | Goodale et al. (2021). *ELife*. https://doi.org/ | 12 | 12 | 21-33 | 6 |

| | | | | | | | |
|---|---|---|---|---|---|---|---|
| | | | 10.7554/eLife.62376<br><br>https://doi.org/10.6084/m9.figshare.28225415.v3. | | | | |
| ME-REST-SUPP | Subset | Respiration, PPG | https://openneuro.org/datasets/ds003592/versions/1.0.11<br>**OpenNeuro Accession Number:** ds003592<br>**Version:** 1.0.11 | 87 | 165 | 18 - 34 | 58 |
| HCP-REST | Subset | Respiration, PPG | https://www.humanconnectome.org/ | 30 | 30 | 22-37 | 17 |
| NKI-TASK | Subset | Respiration, PPG, Skin Conductance | http://fcon_1000.projects.nitrc.org/indi/enhanced/ | 50 | 50 | 15-45 | 30 |
| NKI-REST | Subset | Respiration, PPG, Skin Conductance | http://fcon_1000.projects.nitrc.org/indi/enhanced/ | 50 | 50 | 18-45 | 33 |
| NATVIEW-REST | Full | EEG, Pupillometry | (Telesford et al., 2023)<br><br>https://fcon_1000.projects.nitrc.org/indi/retro/nat_view.html | 21 | 33 | 22-51 | 10 |
| YALE-REST | Full | Pupillometry | https://openneuro.org/datasets/ds003673/versions/2.0.1<br><br>**OpenNeuro Accession Number:** ds003673<br>**Version:** 2.0.1 | 27 | 54 | 21-37 | 16 |
| Clamped CO2 | Full | N/A | (Golestani & Chen, 2020) | 13 | 13 | 18-32 | 9 |

Supplementary Table 1. **Dataset Details and Demographics.** Details (manuscript label, signals recorded, reference) and demographics (sample size, age range, sex) for datasets used in this study. Note, demographics are based on the dataset sample after the quality control stage.

## Supplementary Figures

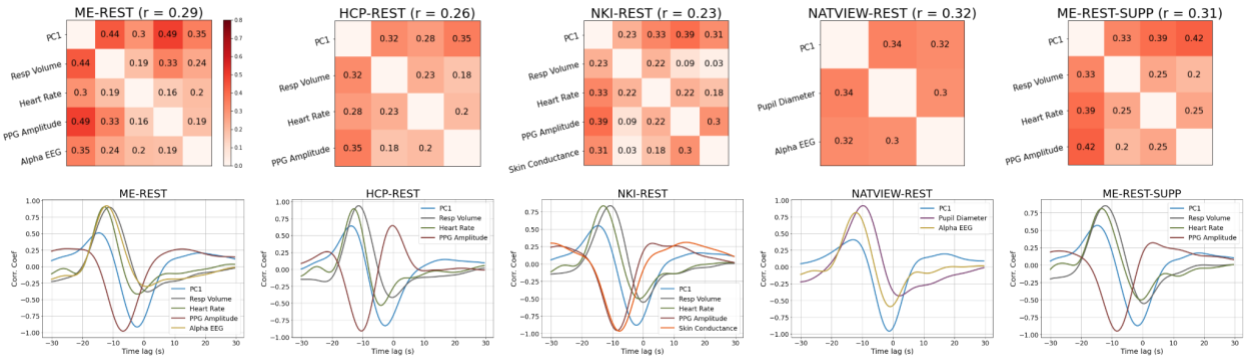


Supplementary Figure 1. **MCCA of Resting-State Datasets and Cross-Correlations. Top panel:** The pairwise correlations (top) between all physiological signals (including the global fMRI signal; PC1) in the first canonical component of the MCCA analysis and their time lags (bottom) for five resting-state datasets, as displayed in **Figure 1**. The average pairwise correlation is displayed beside the title of each correlation matrix. **Bottom panel:** To extract timing information between the signals in this low-dimensional space, we cross-correlated each physiological signal with its projection onto the first canonical component**.** The cross-correlations between each physiological signal and its projection onto the first canonical component are displayed in the bottom panel, where each signal is displayed in a different color. Comparison of the relative timing between peaks of the cross-correlation curves across physiological signals provides the lead-lag relationships between signals within the first canonical component of MCCA.

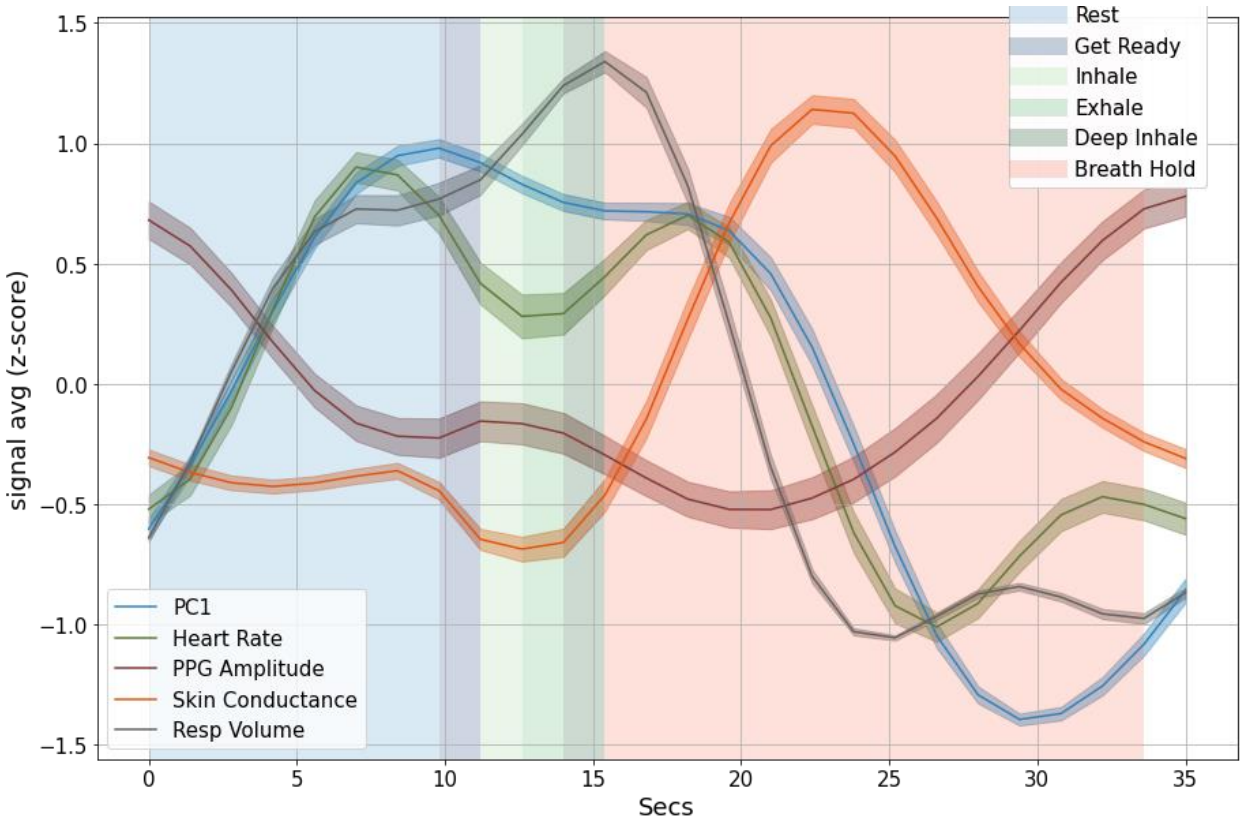


Supplementary Figure 2. **NKI-Breath Hold Task.** Physiological trial averages for a full block of the paced inhalation/breath hold task (NKI-TASK). The shaded regions around the lines represent +- 1 standard error of the mean, which are calculated from cluster bootstrapping ($N_{bootstraps}$ = 500; *see Methods and Materials*). The paced breathing/breath-hold task was a block design consisting of a fixed sequence of rest (10s), a cue (2s) followed by two deep inhalations (6s), and a breath-hold (18s), immediately followed by another sequence. Time points in separate blocks are shaded to distinguish activity in each block: rest (10s duration; blue), 'get ready' cue (2s; dark blue), inhalation (2s; light green), exhalation (2s; medium green), deep inhalation (2s; dark green) and breath hold (18s; red).The physiological dynamics of the paced breathing/breath hold task (NKI-TASK) are more complex than those observed in response to isolated deep inhalations (**Figure 3A**). For example, large increases in respiratory volume are observed during the paced inhalation exercise before the breath hold and the 'rest' blocks that precede the paced inhalation exercise, due to their placement immediately after the breath hold. The timing of the large amplitude peak of global fMRI signals in the rest period (~10s) and following the deep inhalation block (19s) are consistent with the timing of the respiration response peak observed to isolated deep inhalations (**Figure 3A**). Consistent with the response to isolated deep inhalations, an increase in heart rate is observed around the time of the global fMRI peak, shortly followed by peripheral vasoconstriction. In addition, a large amplitude response in skin conductance is observed around the same time as peripheral vasoconstriction. The trough of the global fMRI response, along with peripheral vasodilation, occurs in the latter half of the breath hold block, consistent with the peak-to-trough timing observed in deep inhalations.

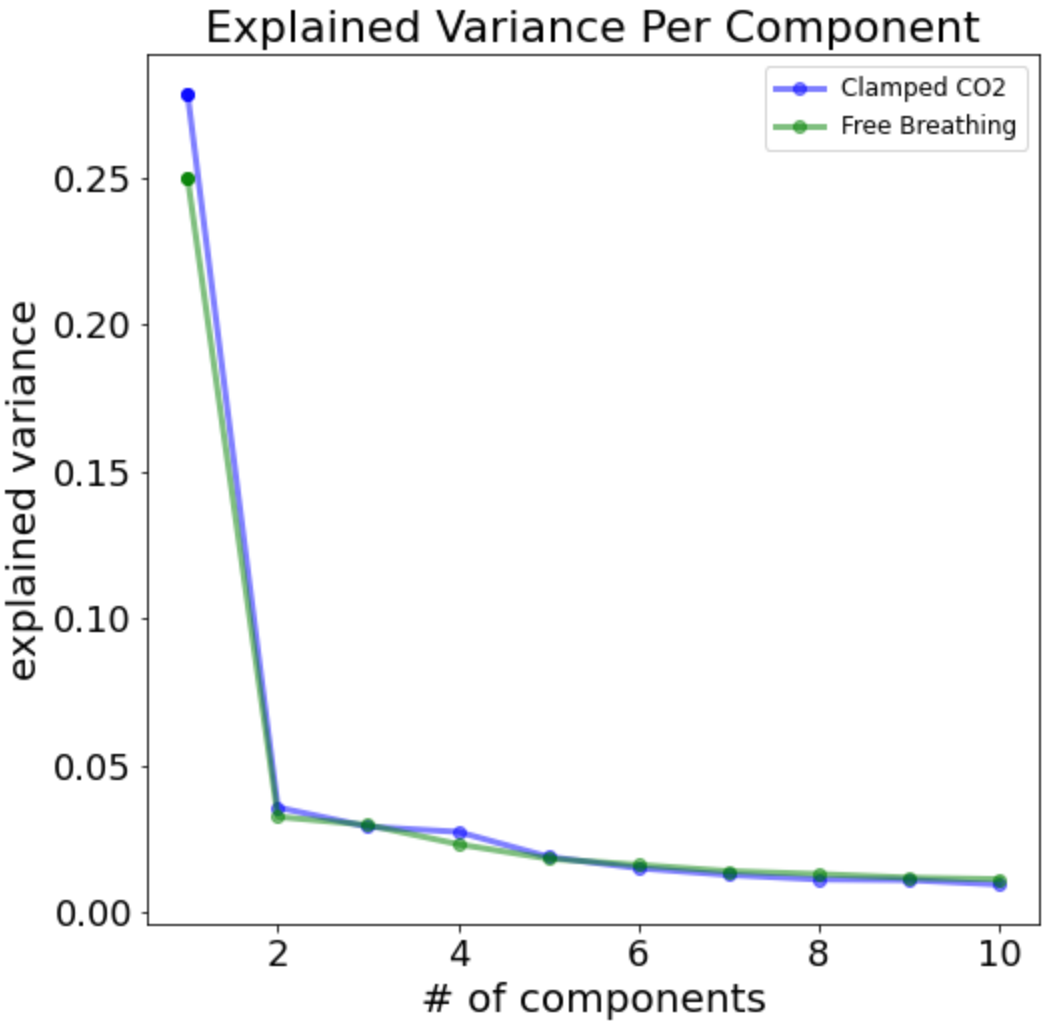


Supplementary Figure 3. **Scree Plot of Eigenvalues for Clamped CO2 and Free Breathing Conditions.** A scree plot of eigenvalues of the first ten components from PCA estimated from the free breathing (green) and 'clamped' CO2 (blue) condition. As can be observed from the scree plot, the low-dimensional structure of fMRI time courses between the two conditions is similar.

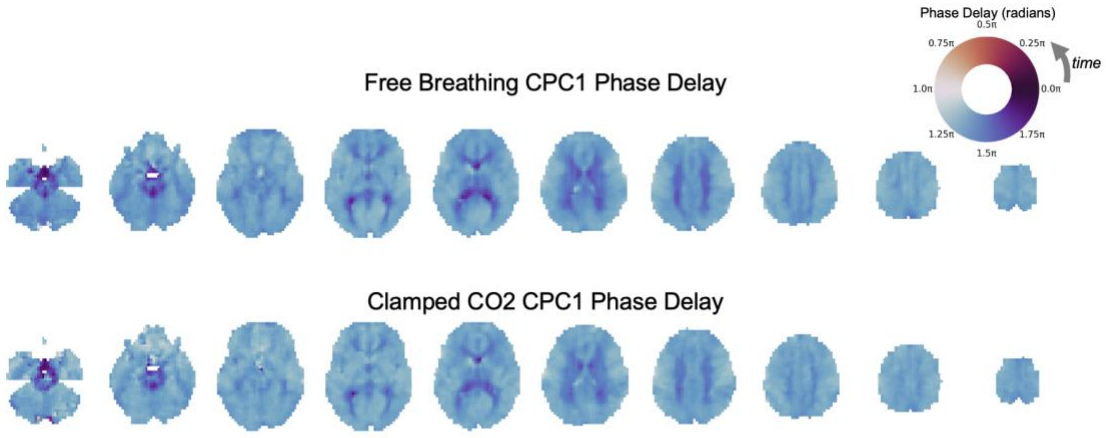


Supplementary Figure 4. **CPC1 Phase Delay in Free Breathing and Clamped CO2 Conditions.** Phase delay maps of the first complex principal component (CPC1) computed from fMRI time courses in free breathing and clamped CO2 conditions. The phase delay map of the first complex principal component encodes the time-delay (in radians) between voxels within the component. Because phase delay is measured in radians (0 to 2pi), they are displayed with a circular color map. As can be observed from the brain maps, the distribution of phase delay values across the brain is highly similar across free breathing conditions and clamped conditions.


Supplementary Figure 5. **Explained Variance of High-Frequency Cardiac Regressors In Multi-Echo ICA Denoised Time Courses.** Brain maps of the group-averaged explained variance ($R^2$) estimates at each voxel by high-frequency cardiac (RETROICOR) regressors. To verify that the spatiotemporal pattern of the global fMRI signal (**Figure 5**) does not arise primarily from aliased cardiac pulsations, we performed regression modeling of (aliased) high-frequency cardiac RETROICOR regressors in Multi-Echo (ME) fMRI data. Specifically, we performed regression modeling on both the ME-ICA denoised time courses and on the time courses that were rejected as echo-time independent 'noise' by ME-ICA (i.e., time courses constructed from the rejected ME-ICA components). As can observed in the group-averaged $R^2$ maps, high-frequency cardiac pulsation effects are primarily observed in the ME-ICA rejected time courses, and are largely attenuated in the denoised time courses.

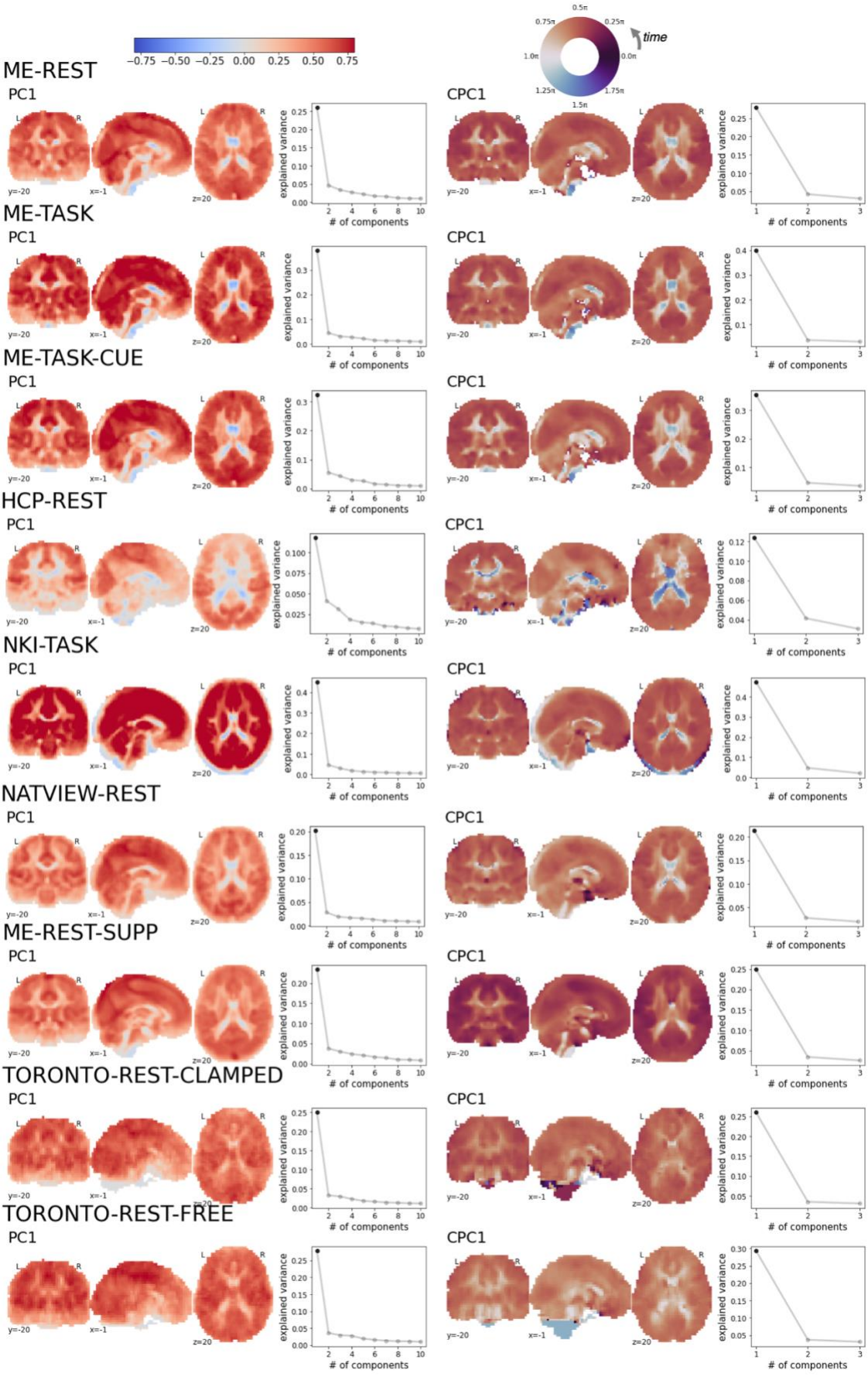
−0.75 −0.50 −0.25 0.00 0.25 0.50 0.75
0.5π
0.75π
0.25π
time
1.0π
0.0π
1.25π
1.75π
1.5π
ME-REST
PC1
CPC1
ME-TASK
PC1
CPC1
ME-TASK-CUE
PC1
CPC1
HCP-REST
PC1
CPC1
NKI-TASK
PC1
CPC1
NATVIEW-REST
PC1
CPC1
ME-REST-SUPP
PC1
CPC1
TORONTO-REST-CLAMPED
PC1
CPC1
TORONTO-REST-FREE
PC1
CPC1
L
R
y=-20
x=-1
z=20
explained variance
# of components

Supplementary Figure 6. **First Principal Component and Complex Principal Component Across Datasets.** Spatial weights of the first principal component (PC1; left) and phase delay maps of the first complex principal component (CPC1; right) across all datasets used in this study. Explained variance plots (Scree plots) are displayed to the right of each brain map displaying the explained variance by the first and subsequent principal components. The phase delay map of the first complex principal component encodes the time-delay (in radians) between voxels within the component. Because phase delay is measured in radians (0 to 2pi), they are displayed with a circular color map.

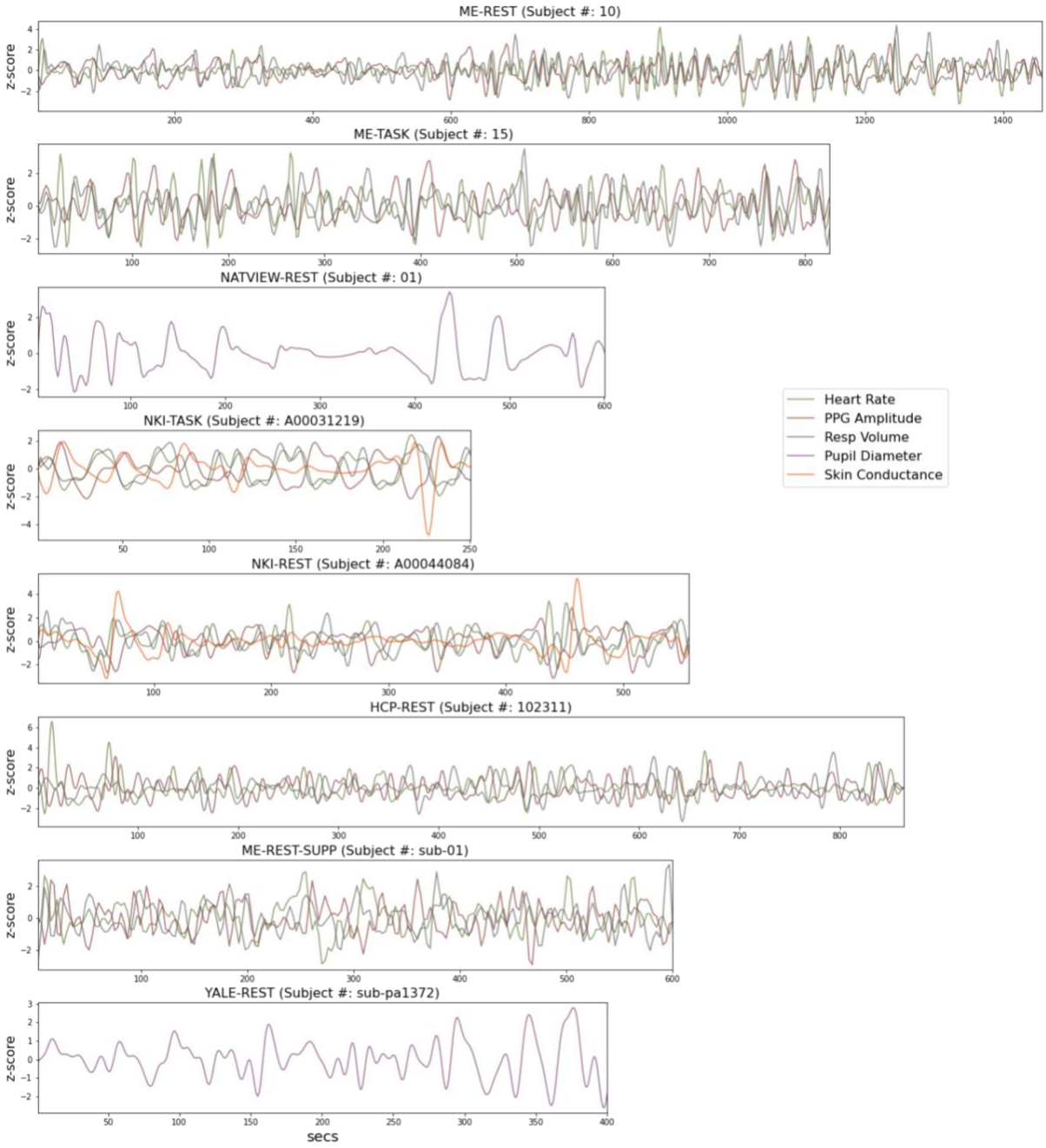


Supplementary Figure 7. **Physiological Time Series from Example Subjects.**

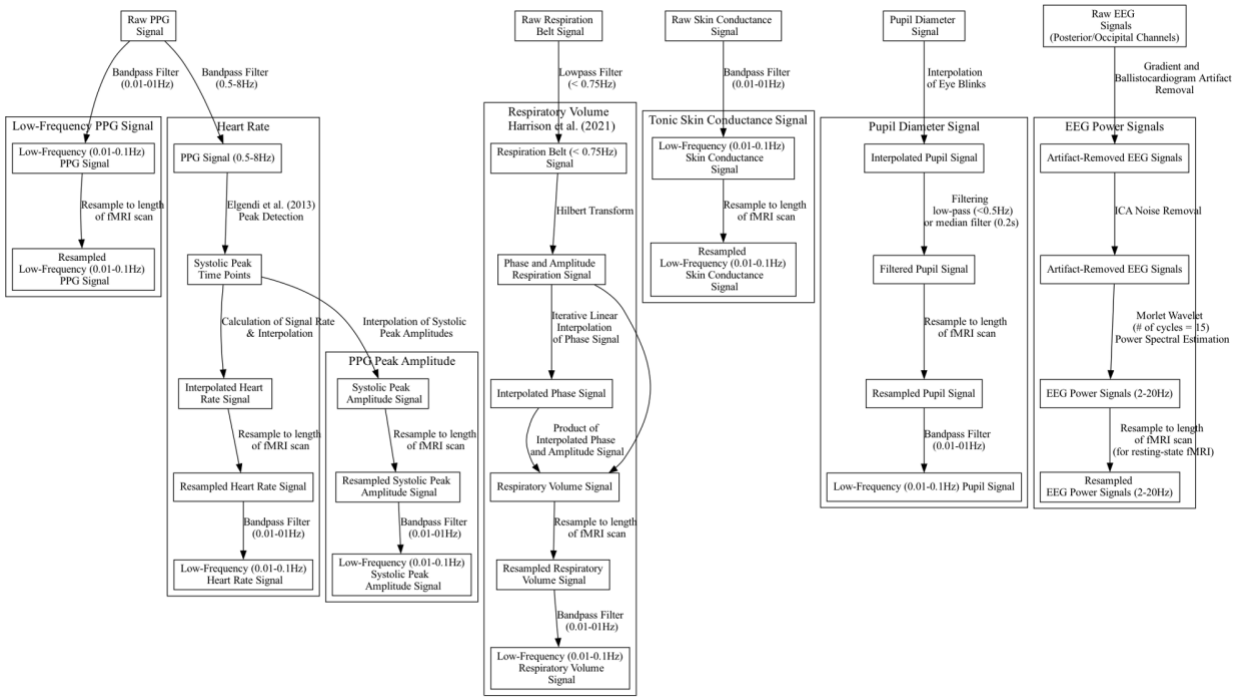


Supplementary Figure 8. **Electrophysiological Signal Preprocessing Pipeline.**

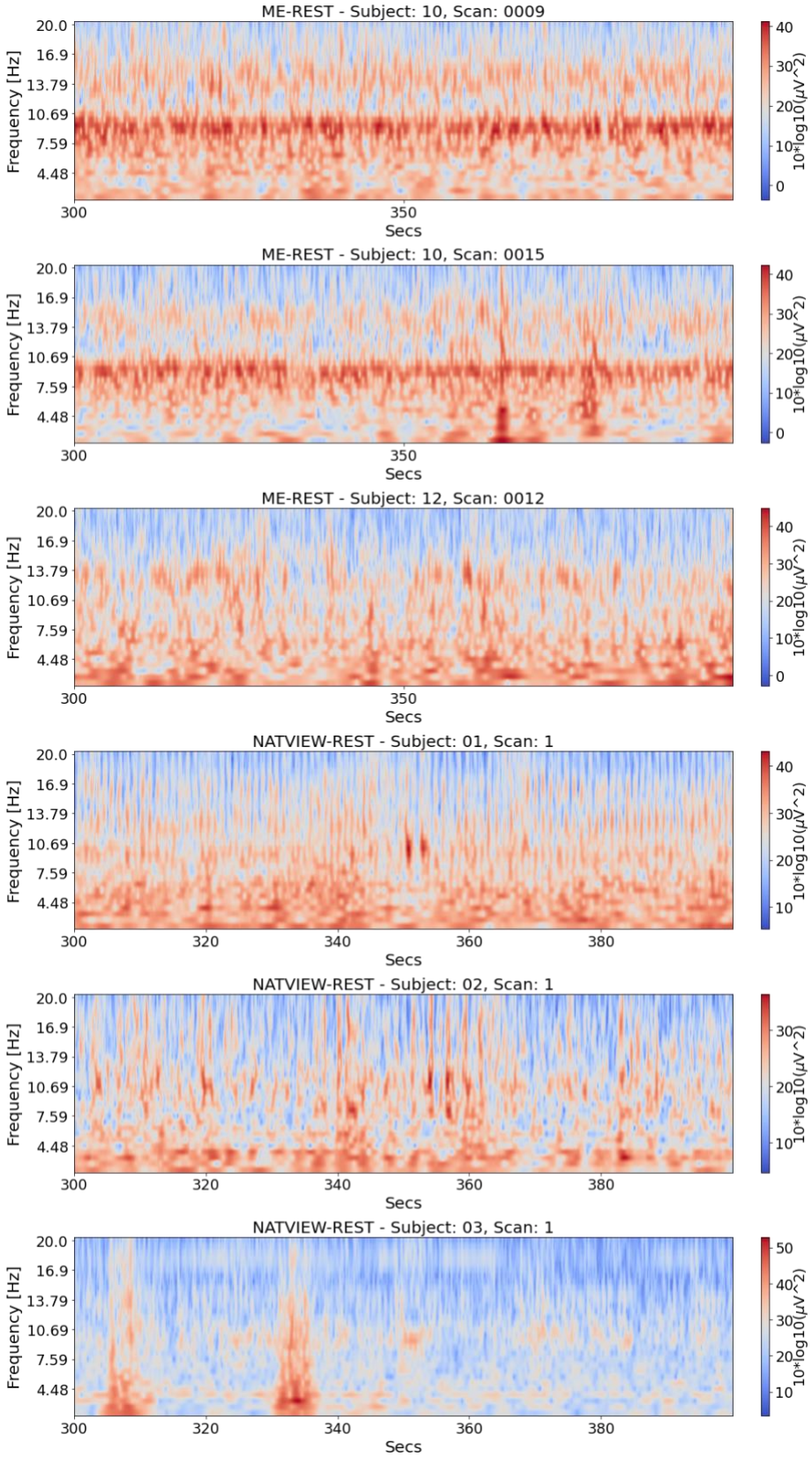


Supplementary Figure 9. **Channel-Averaged EEG Spectrograms Samples from Example Subjects.** EEG time-frequency power plots of sample time points (300 - 400 seconds post scan-onset) averaged

across channels used in the study (posterior and occipital channels). Time-frequency EEG power was extracted via Morlet wavelet filters using the same parameters for analyses presented in **Figure 1** and **Figure 2** (number of cycles = 15; frequencies: 2 - 20Hz).

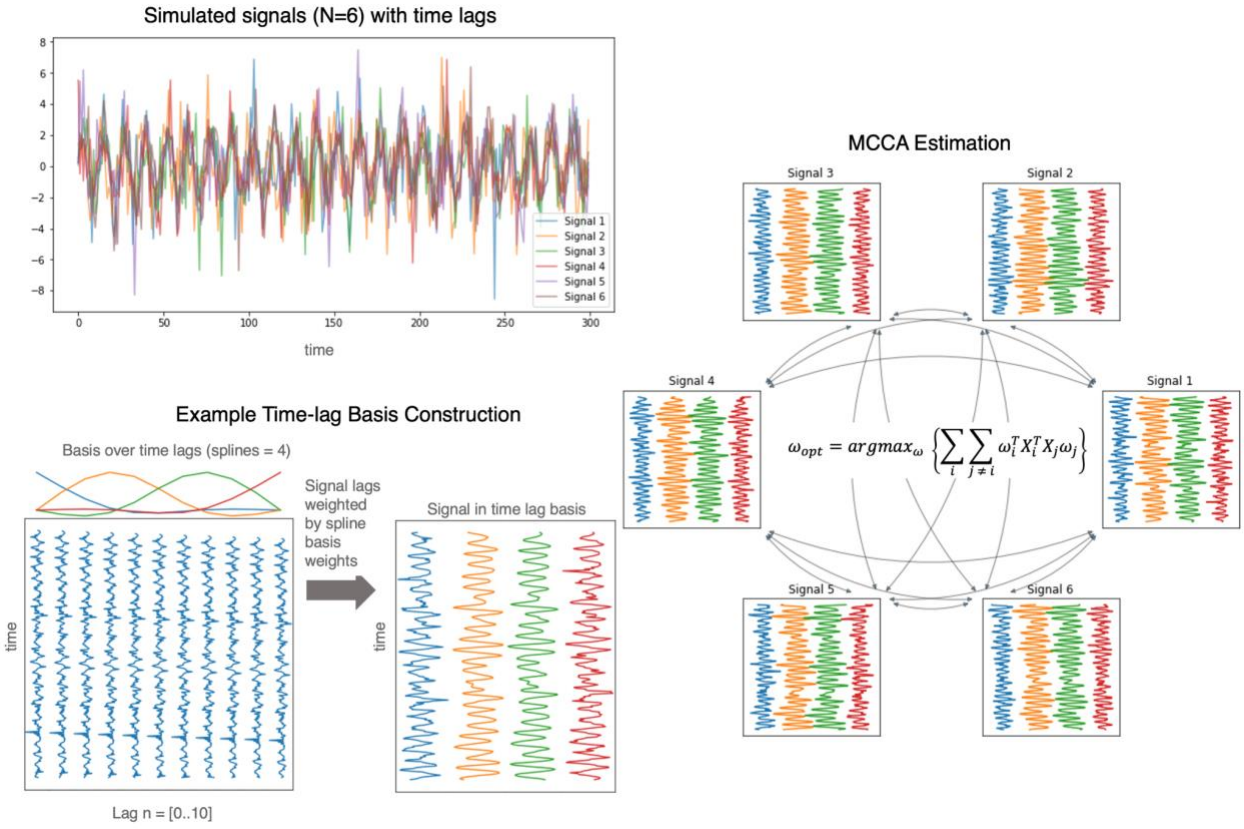


Supplementary Figure 10. **Illustration of Multiset Canonical Correlation Analysis.**

## Supplementary-Only References


68. Smith, S. M. *et al.* Resting-state fMRI in the Human Connectome Project. *Neuroimage* **80**, 144–168 (2013).

69. Gorgolewski, K. *et al.* Nipype: a flexible, lightweight and extensible neuroimaging data processing framework in python. *Front Neuroinform* **5**, 13 (2011).

70. Glasser, M. F. *et al.* The minimal preprocessing pipelines for the Human Connectome Project. *Neuroimage* **80**, 105–124 (2013).

71. Andersson, J., Jenkinson, M. & Smith, S. Non-linear registration, aka spatial normalization. *FMRIB technical report TR07JA2* (2010).

72. Allen, P. J., Josephs, O. & Turner, R. A Method for Removing Imaging Artifact from Continuous EEG Recorded during Functional MRI. *NeuroImage* **12**, 230–239 (2000).